Relationships Between Anhydrite Mineral Lineations and Directions of Megascopic Strain

W.M. Schwerdtner
Department of Geology
University of Toronto
Toronto, Ontario,
Canada

ABSTRACT

In "metamorphic" anhydrite rocks from three evaporite domes, mineral lineations and schistosity normals are correlated with local directions of megascopic *finite strain, deduced for several bending folds, competent buckles, and a boudin. Schistosity seems to develop parallel to the dominant planar discontinuity (bedding or fracture cleavage), but need not be subnormal to the local direction of greatest megascopic shortening. Anhydrite lineations are invariably parallel to the direction of maximum* sectional *extension, along the dominant planar discontinuity.*

Hence mineral lineations in schistose anhydrite can be used as strain-direction indicators in geological mapping. It must be emphasized that trajectories of principal finite extension will generally be somewhat oblique to lineation directions, which reduces their usefulness in structural analysis.

Existing anhydrite lineations may have been bent by flexural slip, or "rigidly" displaced by rotational faulting. However, lineations will always be parallel to sectional extension directions, referred to internal coordinates of rock "specimens," although they may no longer correspond with regional extension directions, referred to geographic coordinates.

INTRODUCTION

The fabric of saline rocks in piercement domes is commonly "metamorphic" (Braitsch, 1962, p. 148), i.e., it is indistinguishable from that of high-grade metamorphic tectonites. Notably the "geschieferte Anhydrit" (schistose anhydrite), bears a marked resemblance to coarsely crystalline amphibolites. In the eastern Alps, units of schistose anhydrite occur in metamorphic silicate rocks of the Val Martello, Ortler-Cevedale Group (Andreatta 1938). The schistosity plane in the anhydrite is parallel to that of the host rock. Apparently, lineation (aligned prismatic grains) and schistosity[1] in both rocks developed under analogous thermodynamic conditions and are oriented parallel to the same directions of megascopic finite strain. Rather than predicting from symmetry relationships whether a principal axis of strain is parallel or normal to the anhydrite lineations (Turner and Weiss, 1963, p. 399), the directions of extreme sectional strain (Ramsay, 1967, p. 158) have been deduced within selected tectonic structures, from the distortional pattern of the predeformational layering. These non-principal directions of finite strain could then be correlated with lineation directions and schistosity normals to determine the nature of their interrelationships. If schistosity and mineral lineations in anhydrite develop under analogous dynamic conditions as those in metamorphic silicate rocks, then the present analysis is of more general importance.

In evaporite domes, compositional layering is generally due to deposition (bedding) (Lotze, 1957, p. 196-198; Braitsch, 1962, p. 117, 193; Schwerdtner, 1967), whereas it may be due to syndeformational metamorphic differentiation in many metamorphic silicate rocks (Ramberg, 1952, p. 215). In order to reconstruct the directions of

1. "Schistosity: that variety of foliation that occurs in coarser grained metamorphic rocks. Generally the result of the parallel arrangement of platy and ellipsoidal mineral grains (Billings, p. 336, 1954)." Glossary of geology and related sciences, 2nd edition. 1960. American Geological Institute.

sectional finite strain it is necessary to have some predeformational surface which can be recognized as such after deformation.

MEGASCOPIC STRAIN DIRECTIONS IN THREE TECTONIC PROTOTYPES

General statement.

In the absence of natural strain gauges, such as ooliths or fossils, local directions of megascopic strain may be inferred from the geometry of simple natural structures. Any simple structure must first be identified with a tectonic prototype that has a definite pattern of heterogeneous strain (for example flexural flow folds). Numerous models of prototypes, containing small strain ellipsoids, have been published in recent years (for instance Ramberg, 1963; Ramsay, 1967). These models show that the principal directions of finite strain are generally oblique to layering, regardless of the magnitude of overall deformation. The trace of intersection between a structural plane (e.g., bedding or cleavage) and a local finite-strain ellipsoid is generally an ellipse, whose longest axis is the "direction of maximum sectional strain" (M), and whose shortest axis is the direction of minimum sectional strain (Ramsay, 1967, p. 158).

In articles of progressive hemogeneous deformation, movement paths of directions of extreme sectional strain are generally referred to the fixed principal axes of bulk strain. The total movement of the strain directions can be resolved into two parts, (1) an "independent" movement on the bedding plane, and (2) a "dependent" movement together with the rotating bedding. Only the former is important in the present analysis of mineral lineations. Within several tectonic prototypes, the local directions of extreme sectional strain do not shift during progressive deformation. This means that M does not move on the bedding plane, i.e., it remains fixed relative to a sectional reference line, for instance a fold hinge. In Flinn's (1962) terminology, this situation corresponds to those cases in which the movement of a given structural element coincides with that of a sectional principal direction. In general, the structural movement path tends to diverge from the "principal" direction movement path on the Wulff net (Flinn, 1962, p. 415).

Tight competent buckles in markedly incompetent host rocks.

Models illustrating the strain distribution in cross sections of tight buckles have been published by Ramberg (1963, Fig. 11) and Ramsay (1967, Fig. 7-68). These figures reveal the three-dimensional strain distribution, provided the bulk deformation is biaxial. Ramberg's model applied to very competent buckles without significant amounts of "homogeneous" strain[2], whereas Ramsay's model contains a considerable amount of homogeneous flattening. During progressive strain, local directions of maximum finite extension tend to approach the cross-sectional trace of the hinge plane, throughout the entire buckle (Fig. 1). M on bedding surfaces is parallel to the hinge line in the crest and in the near limbs, but perpendicular to the hinge line in the far limbs. (The point of change-over from hinge-parallel to hinge-normal depends on the magnitude of homogeneous strain.) The orientation of M does not change in the crest, even if the competent material undergoes large amounts of homogeneous extension parallel to the hinge line, as long as the direction of maximum homogeneous shortening is perpendicular to the axial plane.

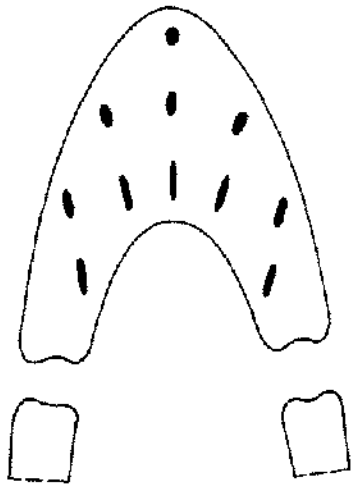

Figure 1. Biaxial strain distribution (schematic) in cross secton of a tight buckle (after Ramsay, 1967, Fig. 7-68). No finite strain parallel to the hinge line.

2. The local finite strain, throughout bending folds, buckling folds, and boudinage structures, can be resolved into a (variable) heterogeneous component and into a (constant) homogeneous component.

Triaxial lenticular boudins.

Voight (1965) has derived equations for calculating average values of finite strain due to cylindrical boudinage. He assumes that the maximum thickness of a boudin (T) corresponds to the predeformational thickness of the component layer (T_o). The cross-sectional area of incipient boudins (A) can then be equated with a predeformational rectangle, whose thickness is $T=T_o$ and whose width (W_o) can be calculated:

$$(1) \qquad W_o = A/T_o.$$

The width of boudins (W) can be readily measured.

Thus the average quadratic elongation (λ_m) is

$$(2) \qquad \lambda_m = (W/W_o)^2 = (WT_o/A)^2.$$

This approach may be extended to all cross sections[3] of triaxial lenticular boudins, regardless if they are due to "double boudinage" or repeated necking. M on bedding may thus be located for a given triaxial boudin.

Finite components of homogeneous strain within incipient triaxial boudins, which cannot be recognized geometrically, alter the necking-shape significantly, and lead in turn to erroneous determinations of M. This possibility may be excluded for incipient triaxial boudins due to "double boudinage" (Flinn, 1962, p. 405).

The average extension for each half of a boudin cross section can be calculated separately; in fact, the average strain of any cross-sectional band can be found (Fig. 2). This procedure can be applied to any layer within a boudin, whose cross-sectional strain distribution can thus be analyzed (Fig. 2). The "principal sections" of triaxial boudins, parallel to their long and intermediate axes (subscripts 1 and i), are of special importance (Figs. 2a, 2b).

Consider a small specimen with lateral faces cut perpendicular to the long and intermediate axes of a "large" triaxial boudin (Fig. 2c). Let the specimen be located near the T,W_i plane (Fig. 2), and have a square base parallel to layering. The megascopic strain varies somewhat throughout the specimen; thus average magnitudes of strain are obtained by the above equations.[4] Because $a_i < a_1$ and $w_i = w_1$, $w_{oi} < w_{o1}$. This means that M is approximately parallel to the projection onto the layering of the intermediate axis of the boudin. If the size of the small specimen is reduced to the domain of a thin section, the state of megascopic strain becomes quasi-homogeneous. Note that M is

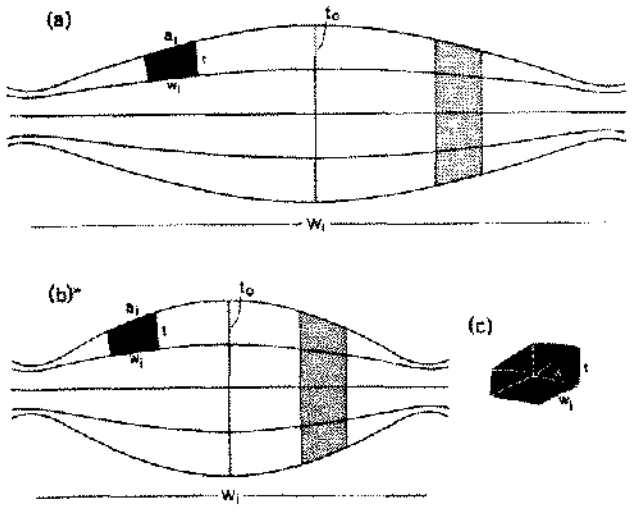

Figure 2. (a,b) Strain analysis in "principal planes" of a triaxial boudin. W_1 = boudin length, W_i = boudin width, t_o = predeformational thickness of a thin unit, t = post-deformational thickness of t_o. w_1, w_i arbitrarily chosen widths of areas a_1 and a_i. (c) t, w_1 w_i = dimensions of a small bedding-parallel element located near the T, W_i plane, and cut parallel to the "principal planes" (T, T_i and T, W_1). $w_1 = w_i$.

not affected by large amounts of dilatation or homogeneous shortening normal to layering ($t_o > t$). However, all strain magnitudes would be relative to an unknown zero.

Figure 3b is a schematic cross section through an incipient boudin, drawn on the basis of field observations (Fig. 3a) and experiments with mild steel (Nadai, 1950, Fig. 19-32). The acute angles of the initially rectangular grid indicate that M is oblique to local directions of maximum finite extension, except at the points of maximum and minimum shortening, and on the central bedding plane.

Bending folds formed under tangential extension.

The strain distribution during bending under lateral extension has been outlined by Ramberg (1955, Fig. 2D). Note that the trajectories of maximum extension are generally oblique to layering, as indicated by the distortion of the orthogonal grid.

3. All extension values are exaggerated, because significant decreases in area occur during any triaxial distortion.

4. Actually, the initial-specimen thickness (t_o) has become somewhat oblique to layering (Fig. 3), i.e., the deformational thickness (t) corresponds to a line initially inclined to layering. Thus the initial specimen was closer to a parallelepiped than to a rectangular box. This does not affect the calculations to w_{o1} or w_{oi}, the basal dimensions of the initial specimen.

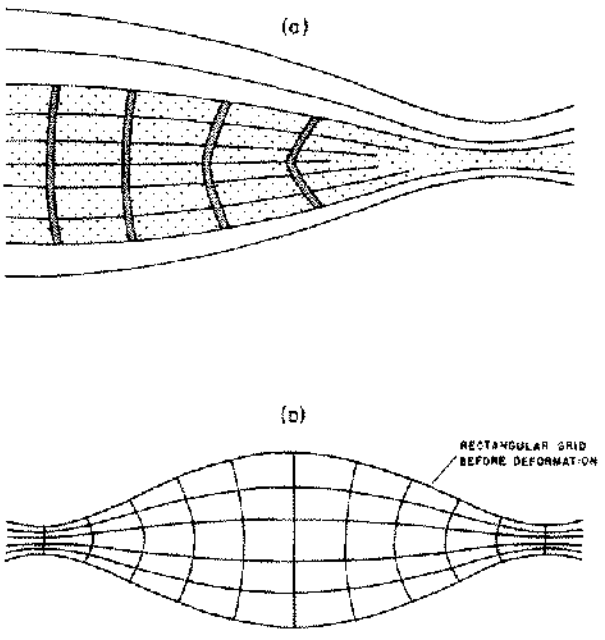

Figure 3. Bedding-parallel shear of healed joints (a) due to necking of limestone bed in anhydrite (South Fiord dome). Early jointing occurred presumably normal to bedding. Schematic pattern of bedding-parallel shear in a cylindrical boudin (b), after Nadai (1950) in part. The distortional lattice is derived from a predeformational grid with uneven spacing of vertical lines.

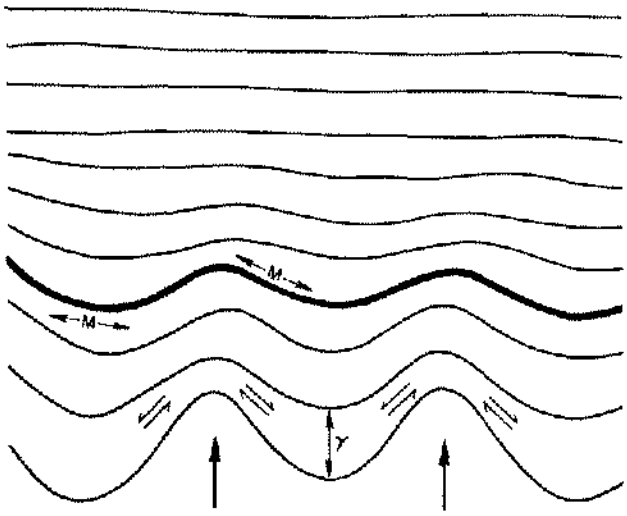

Figure 4. Bending under extension due to diapiric motion (afte Ramberg, 1963, Fig. 2). The deformation is biaxial. δ = ax normal to β, M = direction of maximum sectional strain parallel t bedding.

Because the deformation is two-dimensional, all directions of extreme strain lie in the plane of deformation, i.e., perpendicular to the fold axis. Thinning of beds varies systematically throughout a cylindrical bending fold (Fig. 4). This gives rise to components of shear along the bedding, parallel to the directions of maximum sectional strain (M).

Many natural bending folds have arcuate hinge lines, and some degenerate into domal structures. To facilitate the location of M on bedding surfaces in these non-cylindrical folds, consider them as plane (Turner and Weiss, 1963, Fig. 4-17). The shear components parallel to bedding do not affect M and may be disregarded. Hence only the longitudinal strain components of bending need be discussed.

Like passive folding or "shear folding," bending under tangential extension does not produce an overall shortening or elongation parallel to the initial bedding plane. The displacement of a single bedding surface may thus be approximated by a field of parallel vectors[5].

M forms a radial pattern on a given bed in a domal structure (Schwerdtner, 1963, Fig. 1). An analogous pattern of M chacterizes non-cylindrical plane folds (elongate "domes"), which degenerat into cylindrical plane folds (Fig. 4). Throughou the median cross section of the former folds (Fig 9), M on bedding is parallel to the cross-sectiona trace, where the average tangential extension i maximal. (The median cross section contains th bedding normal at the hinge line culmination, δ and the hinge plane normal.)

Apart from the heterogeneous bending strain most natural structures may also contain larg components of homogeneous strain (for example homogeneous extension of incompetent bed adjacent to triaxial boudins). These may be dif ficult to recognize, but can effect considerable al terations in the pattern of M.

ANHYDRITE RODS IN WINNFIELD SALT DOME

In the Winnfield salt dome, Louisiana, thi anhydrite beds (< 2cm), containing small amount of salt, have been tightly buckled and severel boudinaged. The competent anhydrite beds wer disrupted parallel as well as perpendicular to th fold hinges (Fig. 5). This type of structure is com mon in metamorphic silicate rocks, where it ha been termed "rodding structure" (Wilson, 1953 Ramsay, 1967, p. 391).

5. In fact, the displacement vectors are subparallel. Their divergenc increases towards the hinge line culmination of bending anticline reflecting the heterogeneous extension of bedding.

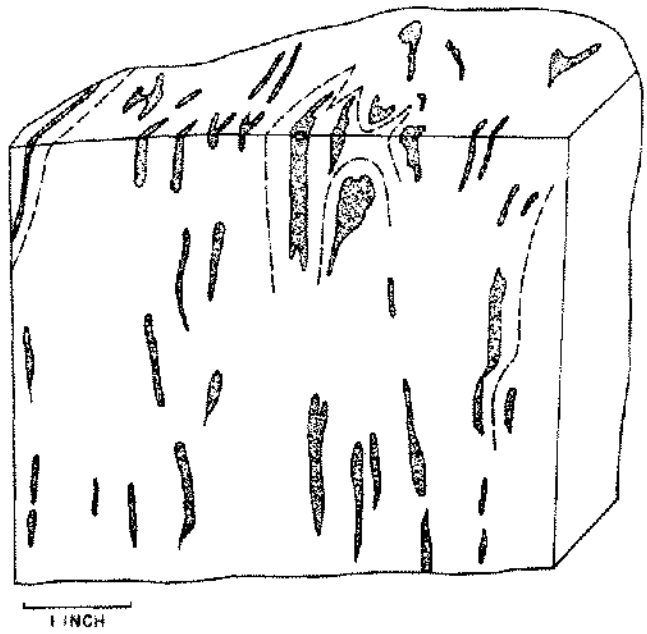

Figure 5. Rodding of white anhydrite units (dotted) in rock salt from Winnfield salt dome. Dashed lines are dark anhydrite stringers.

Balk (1949) observed these anhydrite rods, which he called "pencils" in the Winnfield salt dome, but analysed similar rods in the Grand Saline salt dome, Texas. Apparently, he did not recognize the "rootless buckles," although he noted the tabular shape of the anhydrite inclusions (Fig. 5).

Anhydrite inclusions in Grand Saline dome are usually finegrained (Balk, 1949, Figs. 14-17), so that the lineations must be viewed microscopically. Three point diagrams for the prism axis of anhydrite were published by Balk (1949, Figs. 18-20). In the large hand specimen from Winnfield salt dome (Fig. 5), the anhydrite inclusions have a distinctly visible schistosity and lineation. The mineral lineation is less pronounced in thin sections parallel to bedding, but no microscopic analysis was performed. Anhydrite lineations of individual rods are invariably parallel to the straight hinge lines, whose subvertical attitudes vary slightly throughout the specimen. Lineations in the tabular boudins have the same orientation.

In the hinge portion of the rods, the component of M due to buckling is hinge-parallel. The possibility that the homogeneous strain component of M can be oblique to the hinge line can be excluded because the folds are very tight, and the imaginary line connecting the centers of adjacent boudins is generally parallel to the boudins themselves (Fig. 5). Both observations indicate that the principal direction of bulk finite shortening is nearly perpendicular to the hinge plane, i.e., the component of finite simple shear on the hinge plane must be small (Gay, 1968). The competent anhydrite layers may have been disrupted after the small folds had become nearly isoclinal, with the hinge plane perpendicular to the direction of maximum bulk shortening. Under that condition, no rotation of the boudins with respect to bedding can occur (Gay, 1968; Ramsay, 1967, Fig. 3-46). Alternatively if boudinage had been completed at an earlier stage of folding, most rotated boudins (Ramsay, 1967, Fig. 3-50) would have virtually caught up with the rotated layering surface, after it had become parallel to the hinge plane. This would occur during very large magnitudes of bulk deformation, typical of Gulf Coast domes, when the hinge plane normal approaches the direction of maximum bulk shortening. In that orientation, both components of M (one due to buckling, the other due to homogeneous strain) are parallel to the fold axis in the hinge portion of the competent rods.

In summary, M can only be deduced for the hinge portion of anhydrite rods, where it parallels the prominent mineral lineation. Because cross-sections of individual hinges are quite small, the schistosity surface cannot be identified. (It may be parallel to bedding, or else parallel to hinge planes.) In the tabular boudins schistosity is strictly parallel to bedding, i.e., perpendicular to a direction of large finite shortening.

INCIPIENT TRIAXIAL BOUDIN OF ANHYDRITE FROM SOUTH FIORD DOME

Numerous triaxial boudins of limestone have been observed in the exposed anhydrite core of the South Fiord dome on western Axel Heiberg Island, Canadian Arctic (Schwerdtner and Clark, 1967).

Many of these lenticular boudins occur in radial buckling folds, where first-stage necking must have been unilateral.

Incipient boudinage is also observed in banded anhydrite, where it is mainly due to differences in carbonate content. The surface of banding is parallel to bedding (Schwerdtner and Clark, 1967).

An oriented specimen (Fig. 2) from a 40 cm long triaxial boudin in the eastern peripheral zone of the anhydrite core was analysed microscopically (Fig. 6). The schistosity plane is parallel to bedding, and the mineral lineation is parallel to the projection onto bedding of the intermediate axis of

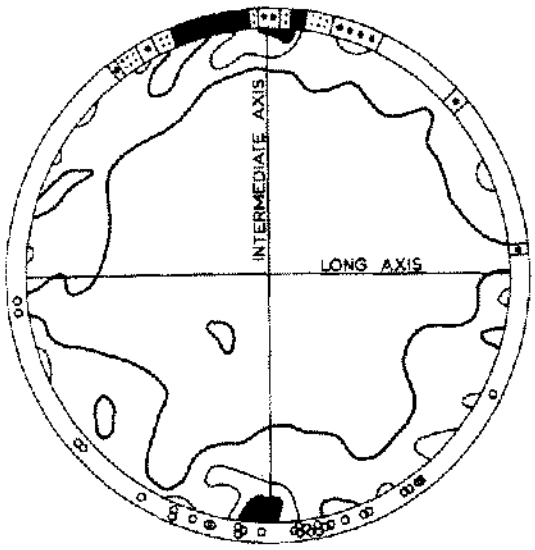

Figure 6. 200 Y-optical (prism) axes of anhydrite from a small domain in the triaxial boudin (Fig. 2c). >5-4-2-0 with 1 percent circle. Apparent long axes of largest grains are plotted in azimuth diagram. Trend of boudin axes on bedding plane (periphery) as shown.

the incipient boudin. The neck thickness in the plane perpendicular to the long axis is somewhat lower than that in the plane perpendicular to the intermediate axis.

As the peripheral zone of the dome is practically free of buckling folds, the present boudin may have been due to multilateral necking. Apparently, the degree of necking was greater parallel to the intermediate axis of the boudin than parallel to its long axis. This suggests that the direction of greatest homogeneous extension along bedding was also parallel to the intermediate axis. Much of this homogeneous extension may have occurred prior to necking. Any later homogeneous extension would tend to make the bedding-parallel section of the triaxial boudin more circular, without changing the direction of maximum bedding-parallel extension due to necking. Thus M should be parallel to the cross-sectional trace (perpendicular to the long axis), even if the component of homogeneous bulk strain was as large as the local heterogeneous distortion.

BENT ANHYDRITE BEDS IN THE BENTHER SALZSTOCK

General statement.

The Benther Salzstock near Hannover, northwestern Germany, has been studied by many geologists (Lotze, 1957, p. 302; Ahlborn and Richter-Bernburg, 1955). Its internal structure is revealed in numerous mine openings, many corresponding to mined-out potash seams. Good exposure and excellent stratigraphic control[6] have permitted detailed underground mapping.

As in the Gulf Coast domes, large flow folds are the dominant structural features (Fig. 7). Due to

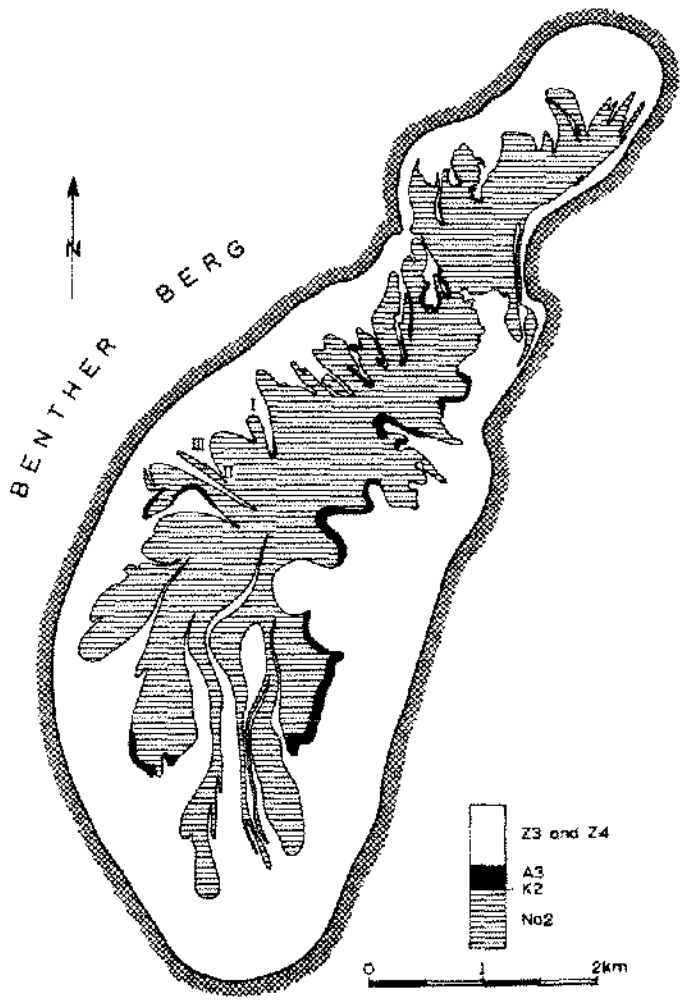

Figure 7. Location of folds I and III in a horizontal section through the Benther Salzstock, 653 m level (after Ahlborn and Richter-Bernburg, 1955). Structure II occurs on the 850 m level.

6. The Zechstein Formation is subdivided into four saline cycles (Richter-Bernburg 1955). The first cycle (Z1) is apparently not involved in doming and can be disregarded. The second cycle (Z2) comprises a thick unit of banded salt (Na2, 600 m thick) overlain by a thin potash seam (K2). The salt rocks of the third and fourth cycles (300 m thick) include several potash seams and numerous interbeds of shale or anhydrite of variable thickness. Much of the rock salt contains large amounts of clay, anhydrite and kieserite. As a whole, it has a higher density and is also more competent than the banded rock salt (Na2).

the marked lithological differences, large buckling folds might be expected, but are apparently rare, in the Benther Salzstock. The mechanism of folding is revealed by the thickest unit of anhydrite (A3). This anhydrite is generally found in the troughs of synclines, but has been severely boudinaged and/or thinned in the fold limbs and near the anticlinal hinges. The overall tangential strain *due to folding* was tensile rather than compressive (Lotze, 1957, Fig. 171). This evidence fits "rheid" folding (Carey, 1954) rather than buckling. Apparently, the salt became diapiric toward the anhydrite bed (A3), during progressive doming. Under these conditions, competent anhydrite beds are bent under extension, and the above model applies (Fig. 4).

Although the crests of most plunging anticlines tend to be free of anhydrite (A3), some do contain considerable amounts (Fig. 7). Thus the present author doubts that buckling-strain can be entirely disregarded. Even anticlines without anhydrite may have been initiated by buckling, in the early stages of doming.

Schistosity in anhydrite.

The most prominent anhydrite unit (A3, 33m thick) is poorly bedded, except for the uppermost portion, which consists of a thin layer of argillaceous anhydrite ("Tonlage," 5 cm) overlain by a layer of light-grey anhydrite ("Anhydritschale," 15 cm). Several of the thinner anhydrite units (less than 5 m), generally poorly bedded, are also composed of a structureless argillaceous layer ("Tonfuss") and a light-colored main portion. It may contain a certain amount of rock salt.

The prominent unit (A3) tends to be fragmented, rather than continuously deformed. A dark banding is developed where the unit has been markedly thinned (up to 90 percent in northwestern parts of the dome). This banded rock is invariably schistose, banding and schistosity being parallel to the anhydrite/salt interfaces, i.e., parallel to bedding. The bedding plane is also indicated by dark laminae in the salt. Gradations exist between distinctly banded schist and weakly banded massive rock. Where the anhydrite has been highly extended, the dark argillaceous layer is markedly thinner, and has locally been boudinaged.

The other anhydrite units tend to deform in a more ductile fashion, as indicated by similar type folds, heterogeneous thinning, etc. Nevertheless numerous fractures can be observed in most exposures. Apart from a major rupture (filled with secondary minerals) between the Tonfuss and the light-colored portion, three types of fractures occur: healed fractures oblique to bedding in the light-colored portion (1), closely-spaced "ductile" fractures parallel to bedding in the Tonfuss (2), and late joints cutting or offsetting the other discontinuities (3). The latter are relatively rare, and shall be disregarded. Fractures of the first type, i.e., thin veinlets of salt or fine-grained carbonates, are very common. These parallel veinlets are evenly spaced (5 to 7 cm), and appear to represent a healed fracture cleavage. The bedding is rarely offset by finite slip on these cleavage planes, nor have they been commonly distorted.

Schistosity is usually confined to the light-colored portion of the anhydrite units, where it is invariably parallel to the veinlets, i.e., oblique to the structureless Tonfuss. In some exposures the Tonfuss itself is fractured and schistose. However, many anhydrite layers with oblique veinlets and/or fractured Tonfuss are not schistose. Thus schistosity may well be an effect rather than the cause of fracturing.

Directions of megascopic strain in folds.

Attitudes of anhydrite lineations in three large folds (Fig. 7) were measured directly, and/or obtained by microscopic analysis (Schwerdtner, 1961; 1964). In view of the mechanical complexity, the geometry of each fold shall be discussed, before deducing directions of megascopic strain.

All tight folds in the Benther Saltzstock are non-cylindrical (Lotze, 1957, p. 306), in fact, many resemble elongate domes rather than plunging folds (Ahlborn and Richter-Bernburg, 1955). Distortion of anhydrite beds in the domal folds can be due to buckling (Ramberg, 1959, Fig. 10; Flinn, 1962), bending under extension, or a combination of both mechanisms. Although buckling folds with arcuate hinges are indicative of some compressive strain parallel to the hinge, M on the fold limbs will tend to fall into the cross-sectional plane (Fig. 1), as in many non-cylindrical bending folds.

Folds I and II (Fig. 8), only exposed in their limbs, represent perfect examples of tight non-cylindrical folds. Fold II has an elliptical cross section, in which β axes can be constructed at the locations of maximum horizontal curvature. One of the bisectrices of the β axes approximates the central axis (δ) of the domal syncline (Fig. 9). Thus the fold geometry is sufficiently defined for constructing the cross-sectional plane. In any adjacent exposure, M deviates from the trace of inter-

section between bedding and cross section such that it assumes its proper radial orientation. The anhydrite lineations, obtained at three single exposures of the prominent anhydrite unit (A3), are apparently parallel to the local M (Fig. 8, 9).

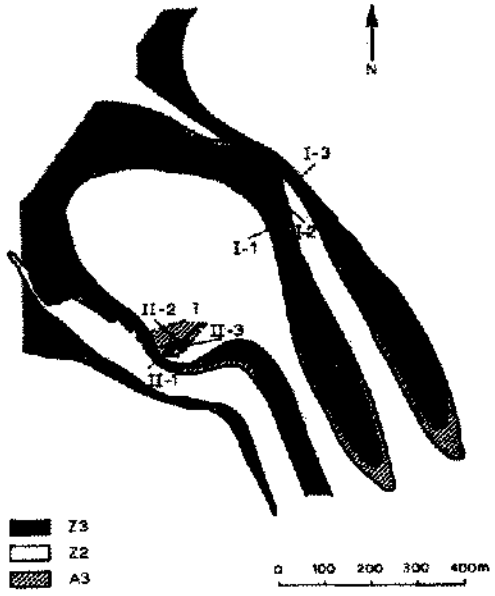

Figure 8. Exposures I-1, I-2, I-3, of fold I on the 653 m level (see Fig. 7), and exposures II-1, II-2, II-3 of fold II (dashed outline on the 850 m level).

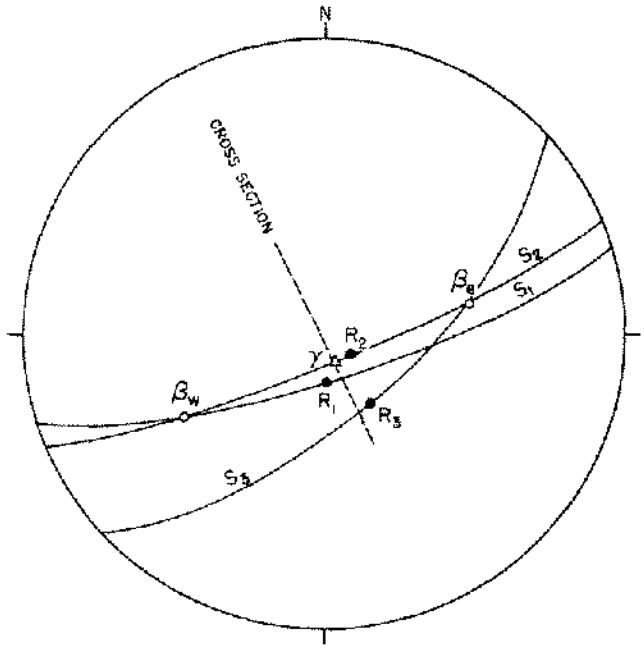

Figure 9. Synoptic diagram for fold II (Fig. 7). S = bedding, R = anhydrite lineations. Suffixes refer to exposures in fold II (Fig. 8). β_e = β axis at eastern hinge, β_w = β axis at western hinge, δ is their subvertical bisectrix. Orientation of cross-sectional plane of fold II as indicated.

The hinge line of fold I (Fig. 8) has only a slight curvature, so that δ is approximately perpendicular to it (Fig. 4). Because the folds are isoclinal, M will be subparallel to δ in the fold limbs. M may also be inferred from boudinage of the thin argillaceous layer ("Tonlage"). Mineral lineations in the three exposures at the 653 m level are practically parallel to M (Schwerdtner, 1961, Appendix). Magnitudes and directions of homogeneous bulk strain in the folded anhydrite cannot be estimated, and must be disregarded. Because the accuracy of determining the component of M due to bending is comparatively low in these large structures, and the anhydrite (A3) is very competent, a consideration of the component of homogenous bulk strain may not be warranted.

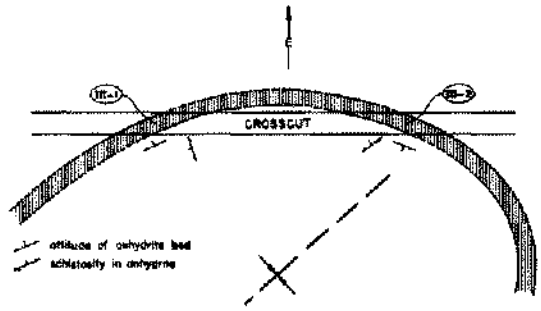

Figure 10. Exposures III-1 and III-2 of the anhydrite bed in fold III on 653 m level (see Fig. 7). Trend and location of hinge surface (known from potash mining) as indicated.

Near the hinge of fold III (Fig. 10), an undisrupted anhydrite unit (3 m thick) is twice exposed in a crosscut. Schistosity is developed in the main portion of the unit, where it is parallel to healed cleavage and oblique to bedding. The orientation of the mineral lineations with respect to the main structural elements is shown in Figure 11. Schistosity is clearly oblique to the hinge surface of the syncline (Fig. 7) but contains a β axis constructed from the bedding attitudes in the two exposures (Fig. 10). This axis should not be parallel to the actual hinge, because folding is noncylindrical. The plunge of an adjacent potash seam suggests that the hinge line of the anhydrite bed is somewhat steeper than β (Fig. 11). Thus the true hinge plane will lie within the stippled area. The present attitude of the cleavage traces is compatible with shear or extension fracturing due to

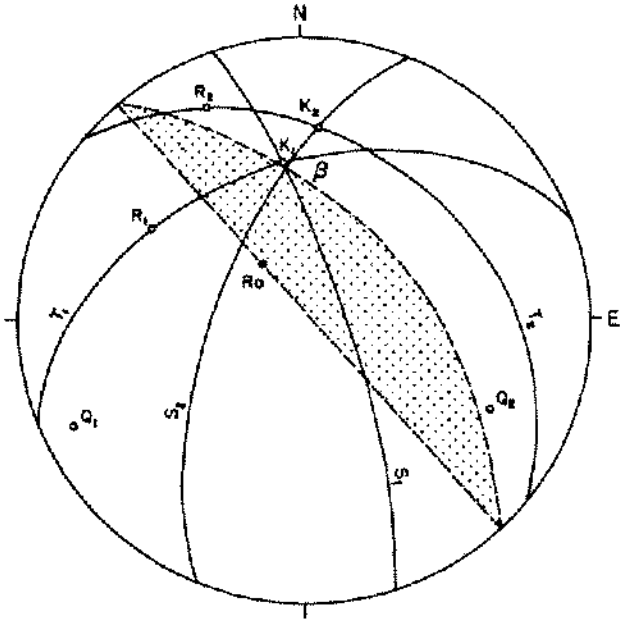

Figure 11. Synoptic diagram for fold III. Elements of exposure III-1 have suffix 1, those of III-2 have suffix 2 (Fig. 10). S = bedding, T = schistosity parallel to fracture cleavage, K = lines of intersection between S and T. Q = normals to bedding. R = anhydrite lineations, β = β axis between S_1 and S_2 Ro = plunge of hinge line of Ronnenberg seam.

buckling as well as bending under extension[7]. However, large amounts of slip have definitely occurred on the cleavage surfaces, which may have been accompanied by a rotation of the cleavage itself.

In exposure III-1, bedding is subparallel to the hinge "plane" whereas the healed cleavage is approximately normal to bedding. As finite thinning of limbs is characteristic for tight buckling as well as for bending under extension, the cleavage normal cannot be parallel to a direction of finite shortening. The same argument can be advanced for exposure III-2, provided deformation was due to bending under extension.

The prominent anhydrite bed (A3) is totally absent in the anticlinal crests adjacent to fold III (Fig. 7). Thus the initial-buckling strain in rather continuous anhydrite layers should be relatively small, and may be neglected. Fracture cleavage may well have been formed during buckling, so that the strain responsible for the schistosity is chiefly due to bending under extension. This type of bending is characterized by differential thinning of beds, whereby the local directions of principal finite shortening tend to be "subnormal" to bedding. In Figure 11, Q_1 and Q_2 lie near the corresponding cleavage planes, i.e., M on the cleavage must subtend large angles with these bedding normals. The angle between R_1 and Q_1 is about 60°, and the angle between R_2 and Q_2 is about 70 degrees. This corresponds with a large component of finite shear in the fold limb, and a somewhat smaller component near the hinge. A more accurate determination of M would require detailed knowledge of the fold geometry, as well as information about the directions of the principal components of homogeneous bulk strain.

SUMMARY AND CONCLUSIONS

Schistosity and mineral lineations develop parallel to the dominant discontinuity plane (bedding or fracture cleavage). In all structures investigated, lineations are parallel to deduced directions of greatest sectional strain (M) but generally oblique to the local principal axes, in domains whose thickness greatly exceeds the spacing between neighbouring discontinuities. This qualification is necessary, because the gross strain of stratified (discontinuous) beds can be markedly different from the strain of thin slices within the bed (see for example Ramsay, 1967, Fig. 7-74). All strain directions inferred above relate to the bulk deformation of (statistical) continua.

Whereas the component of M due to heterogeneous megascopic strain can be readily deduced in competent buckles, lenticular boudins, and bending folds; that corresponding to the homogeneous bulk strain is difficult to predict. Wherever M was actually reconstructed it proved to be a direction of extension. Thus the anhydrite lineations were found to be parallel to the direction of greatest finite extension within that structural surface dominant on a small scale. In most of these structures, schistosity normals are directions of large finite shortening; but they correspond to directions of finite extension in at least one exposure. This is to be expected if discontinuity surfaces rotate during progressive strain.

Hence anhydrite lineations seem suitable as strain-direction indicators in macroscopic structural analyses. Schistosity normals, on the other hand, do not appear to qualify in this respect. Because existing anhydrite lineations may have been rotated in a quasi-rigid fashion, notably by rotational faulting or flexural-slip folding, lineation

7. An earlier interpretation of this cleavage (Schwerdtner, 1964) was based on an inappropriate model.

directions (i.e., directions of greatest sectional extension) should be referred to "specimen coordinates" rather than to the earth's surface. The latter reference frame is invariably employed in the field, when trend and plunge values of lineations are recorded. However, only where late rigid-body rotations can be disregarded, may lineation attitudes be used in reconstructing trajectories of M or directions of regional deformation. Conversely, the continuous variation of lineation attitudes throughout a macroscopic domain need not be due to folding of lineations, but may reflect the original strain distribution in the domain.

ACKNOWLEDGEMENTS

The field measurements were made from 1958 to 1963, while the author was doing doctoral research in the Kaliforschungsinstitut, Hannover, and was subsequently holding a post-doctoral fellowship of the National Research Council of Canada. Some laboratory research was done at the Department of Geological Sciences, University of Saskatchewan, Saskatoon. Thanks are due to Drs. A.R. Berger, University of Toronto and B. Voight, Pennsylvania State University, for criticizing the manuscript. Drs. M.R. Stauffer, University of Saskatchewan, and W.T. Holser, Chevron Research Corporation, La Habra, California, read an earlier version of the manuscript.

REFERENCES

Ahlborn, O., and Richter-Bernburg, G., 1955, Exkursion zum Salzstock Benthe mit Befahrung der Kaliwerke Ronnenberg und Hansa: Z. deutsch. geol. Ges., v. 104, p. 855-865.

Andreatta, C., 1938, Analisi stutturali di rocce metamorfiche. VII: Anidrite: Periodico Mineralogia, v. 9, p. 305-321.

Balk, R., 1949, Structure of Grand Saline dome, van Zandt County, Texas: Am. Assoc. Petroleum Geologists Bull., v. 33, p. 1791-1829.

Braitsch, O., 1962, Entstehung und Stoffbestand der Salzlagerstätten: Berlin, Springer-Verlag, 232 p.

Carey, S.W., 1954, The rheid concept in geotectonics: Geol. Soc. Australia Jour., v. 1, p. 67-117.

Flinn, D., 1962, On folding during three-dimensional progressive deformation: Geol. Soc. London Quart. Jour., v. 118, p. 385-433.

Gay, N.C., 1968, Pure shear and simple shear deformation of viscous fluids. 1. Theory: Tectonophysics, v. 5, p. 211-234.

Lotze, F., 1957, Steinsalz und Kalisalze, I. Teil: Berlin, Bornsträger Verlag, 465 p.

Nadai, A., 1950, Theory of flow and fracture of solids: New York, McGraw-Hill, 572 p.

Ramberg, H., 1952, The origin of metamorphic and metasomatic rocks: University of Chicago Press, 317 p.

——, 1959, Evolution of ptygmatic folding: Norsk Geol. Tidsskr;. v. 39, p. 99-152.

——, 1963, Strain distribution and geometry of folds: Geol. Inst. Univ. Uppsala Bull., v. 42, p. 1-20.

Ramsay, J.G., 1967, Folding and fracturing of rocks: New York, McGraw-Hill 568 p.

Richter-Bernburg, G., 1955, Stratigraphische Gliederung des deutschen Zechsteins: Z. deutsch. geol. Ges., v. 104, p. 843-854.

Schwerdtner, W.M., 1961, Korngefügeuntersuchungen an Anhydritgesteinen im Benther Salzstock (Werk Ronnenberg) bei Hannover: Kali u. Steinsalz, v. 3, p. 173-182.

——, 1963, Petrofabric analysis of some anhydrite rocks, *in* Symposium on salt: Northern Ohio Geol. Soc., p. 249-262.

——, 1964, Gefügestudien an Anhydritbänken im Benther Salzstock (Werk Ronnenberg): Kali u. Steinsalz, v. 4, p. 64-70.

——, and Clark, A.R., 1967, Structural analysis of Mokka Fiord and South Fiord domes, Axel Heiberg Island. Canadian Arctic: Canadian Jour. Earth Sci., v. 4, p. 1229-1245.

Turner, F.J., and Weiss, L.E., 1963, Structural Analysis of metamorphic tectonites: New York, McGraw-Hill, 545 p.

Voight, B., 1965, Boudinage: A natural strain and ductility gauge in deformed rocks (abs.), *in* Abstracts for 1965: Geol. Soc. America Spec. Paper 87, p. 213-214.

Wilson, G., 1953, Mullion and rodding structure in the Moine Series of Scotland: Geologists Assoc. Proc., v. 64, p. 118-151.